Stochastic hybrid model of spontaneous dendritic NMDA spikes

2014 Phys. Biol. 11 016006

(http://iopscience.iop.org/1478-3975/11/1/016006)

IOP Publishing Physical Biology
Phys. Biol. 11 (2014) 016006 (13pp) doi:10.1088/1478-3975/11/1/016006

Stochastic hybrid model of spontaneous dendritic NMDA spikes

Paul C Bressloff[1,3] **and Jay M Newby**[2]

[1] Department of Mathematics, University of Utah, Salt Lake City, UT 84112, USA
[2] Mathematical Biosciences Institute, Ohio State University, Columbus, OH, USA

E-mail: bressloff@math.utah.edu and newby.23@mbi.osu.edu

Received 13 August 2013, revised 13 December 2013
Accepted for publication 20 December 2013
Published 29 January 2014

Abstract

Following recent advances in imaging techniques and methods of dendritic stimulation, active voltage spikes have been observed in thin dendritic branches of excitatory pyramidal neurons, where the majority of synapses occur. The generation of these dendritic spikes involves both Na^+ ion channels and M-methyl-D-aspartate receptor (NMDAR) channels. During strong stimulation of a thin dendrite, the resulting high levels of glutamate, the main excitatory neurotransmitter in the central nervous system and an NMDA agonist, modify the current-voltage (I–V) characteristics of an NMDAR so that it behaves like a voltage-gated Na^+ channel. Hence, the NMDARs can fire a regenerative dendritic spike, just as Na^+ channels support the initiation of an action potential following membrane depolarization. However, the duration of the dendritic spike is of the order 100 ms rather than 1 ms, since it involves slow unbinding of glutamate from NMDARs rather than activation of hyperpolarizing K^+ channels. It has been suggested that dendritic NMDA spikes may play an important role in dendritic computations and provide a cellular substrate for short-term memory. In this paper, we consider a stochastic, conductance-based model of dendritic NMDA spikes, in which the noise originates from the stochastic opening and closing of a finite number of Na^+ and NMDA receptor ion channels. The resulting model takes the form of a stochastic hybrid system, in which membrane voltage evolves according to a piecewise deterministic dynamics that is coupled to a jump Markov process describing the opening and closing of the ion channels. We formulate the noise-induced initiation and termination of a dendritic spike in terms of a first-passage time problem, under the assumption that glutamate unbinding is negligible, which we then solve using a combination of WKB methods and singular perturbation theory. Using a stochastic phase-plane analysis we then extend our analysis to take proper account of the combined effects of glutamate unbinding and noise on the termination of a spike.

Keywords: stochastic ion channels, spontaneous action potentials, WKB, first passage times, excitability

1. Introduction

It has been known for more than twenty years that the dendrites of cortical neurons do not simply act as passive electrical cables but also support a variety of active physiological processes [1]. For example, thick apical dendrites of pyramidal neurons express voltage-gated Na^+, K^+ and Ca^{2+} channels, which support the back-propagation of action potentials (APs) from the soma into the dendritic tree [2, 3]; back-propagating APs are thought to play an important role in spike-timing dependent synaptic plasticity [4]. In addition, sufficient local stimulation of active apical dendrites can initiate regenerative membrane depolarizations known as *dendritic spikes* [5, 6]. Some dendritic spikes are restricted to the local initiation zone rather than invading the cell body, and are thus well placed to mediate the long-term potentiation of synaptic inputs in the absence of output spiking of the neuron [7]. On the other hand, Ca^{2+} APs initiated in apical dendrites

[3] Author to whom any correspondence should be addressed.

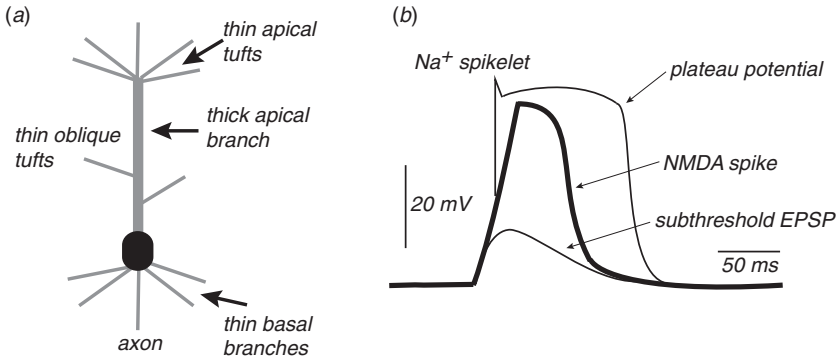

Figure 1. (*a*) Schematic illustration of a pyramidal neuron showing the thick apical dendrite and various thin dendrites. The latter support the initiation of dendritic NMDA spikes. (*b*) Typical waveform of a dendritic NMDA spike. Weak glutamatergic inputs generate EPSP-like (subthreshold) depolarizations. A stronger input can trigger a dendritic plateau potential, consisting of a rapid onset that is often associated with a Na^+ spikelet, a long-lasting plateau phase that can have a duration of several hundred ms, and a sudden collapse at the end of the plateau phase. The plateau potential consists of several dendritic conductances, the most predominant being due to NDMAR channels. Pharmacologically blocking Na^+ and Ca^{2+} channels reveals the pure dendritic NMDA spike [9].

can propagate toward the soma, which provides a mechanism for actively amplifying the effects of distal synapses on AP generation in the cell body [8]. Following advances in imaging techniques and methods of dendritic stimulation, Schiller *et al* [9] established *in vitro* that active processes can also occur in thin basal and apical dendritic branches of pyramidal neurons, where the majority of synapses occur, see figure 1(*a*). In particular, they found stimulus-evoked dendritic spikes whose major ionic component involved ligand-gated and voltage-gated M-methyl-D-aspartate receptor (NMDAR) channels, see also [10–12] and the review [13]. When glutamate (the main excitatory neurotransmitter in the central nervous system) binds to an NMDAR, it modifies the voltage sensitivity of the corresponding ion channel current, which develops a negative slope conductance due to removal of a magnesium block [14, 15]. This means that in the presence of high levels of glutamate, the current-voltage (I–V) characteristics of an NMDAR channel are very similar to the voltage-gated Na^+ channel. Hence, during strong stimulation of a thin dendrite due to the local uncaging of glutamate or high frequency stimulation of a cluster of synapses, the NMDARs can fire a regenerative dendritic spike, just as Na^+ channels support the initiation of an AP following membrane depolarization. However, the duration of the dendritic spike is of the order 100 ms rather than 1 ms.

A schematic illustration of a typical dendritic spike is shown in figure 1(*b*), which consists of a long-lasting plateau potential together with fast onset and termination. The underlying NMDA spike is revealed by blocking Na^+ and Ca^{2+} channels. How the level of glutamate affects the current-voltage (I–V) curves of dendritic membrane is illustrated in figure 2. Immediately following strong stimulation, the maximum conductance of the NMDARs is high so that the N-shaped I–V curve has only a stable depolarized fixed point corresponding to a self-triggering plateau potential. However, as glutamate starts to unbind, the maximum conductance decreases and two additional fixed points arise via a saddle-node bifurcation: a stable resting state and unstable threshold state. The dendritic membrane is now in a bistable regime, although it remains in the depolarized state in the absence

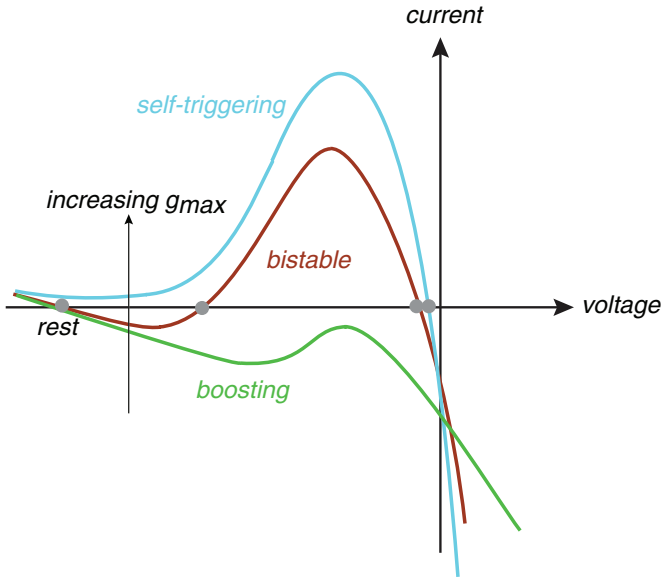

Figure 2. Sketch of current-voltage curves for a dendritic membrane in the presence of glutamate-bound NMDA receptors. The slope of each curve indicates the total voltage-dependent conductance. As the maximum conductance g_{max} of the NMDA channels is increased a family of N-shaped I–V curves is generated with different fixed points. For relatively small g_{max}, the conductance is non-ohmic (boosting regime) but there is only a single fixed point corresponding to the resting state. As g_{max} is increased there is a saddle-node bifurcation resulting in a bistable membrane with a stable resting state and a stable active state separated by an unstable fixed point. For sufficiently large g_{max}, the resting state and unstable fixed point annihilate in a second saddle-node bifurcation resulting in a self-triggering state.

of a hyperpolarizing stimulus. Finally, as the maximum conductance is further reduced, the unstable and depolarized fixed points annihilate in a second saddle-node bifurcation, resulting in a rapid return to the resting state. The I–V curve remains non-ohmic, that is, the current is boosted by active ion channels.

It should be emphasized that dendritic NMDA spikes have not yet been observed *in vivo*, although NMDA-dependent

plateau potentials have been demonstrated in various cells of the spinal cord and brain stem during locomotion [16]. Nevertheless, there have been a number of suggestions regarding the functional role of dendritic NMDA spikes [13]. First, the local nature of the spikes provides a possible mechanism for parallel processing in different branches of the basal dendritic tree. Second, the prolonged duration of NMDA spikes provides a potential cellular substrate for short-term working memory [17, 18] and could also enable neurons to act as 'neural integrators' similar to those found in the oculomotor system [19]. Interestingly, the duration of a plateau potential is proportional to the strength of stimulation. Finally, dendritic spikes close to the soma could help to regulate cortical UP states, which are periods of high synchronous activity that alternate with periods of quiescence during sleep. It has been found in acute brain slice preparations that glutamate-evoked plateau potentials generate sustained depolarizations in the soma of pyramidal neurons, which resemble cortical UP states [13, 20].

There have been a number of computational studies of the voltage dependence of NMDA conductances at the macroscopic level, based on Hodgkin–Huxley-like dynamics [21–24]. Although some of these works explore the contribution of NMDA conductances to bistable membranes, none of them explicitly address the initiation and termination of dendritic NMDA spikes. They also assume that the number of ion channels is sufficiently large so that fluctuations in the opening and closing of the channels due to thermal noise can be ignored. In this paper, we consider a stochastic conductance-based model of active dendritic membrane containing a mixture of glutamate-bound NMDARs and voltage-dependent Na^+ channels, in which the effects of channel fluctuations are taken into account. (For simplicity, we ignore additional voltage-dependent ion channels such as Ca^{2+}.) As with other recent conductance-based models of stochastic ion channels [25–28], our model takes the form of a stochastic hybrid system, in which a piecewise deterministic dynamics describing the time evolution of the membrane potential is coupled to a jump Markov process describing the opening and closing of a finite number of ion channels [26–30]. We focus on the role of ion channel noise on the initiation and termination of spontaneous dendritic spikes, both of which are formulated in terms of an escape problem. One approach to analyzing escape problems for such a system would be to carry out a perturbation analysis in the small parameter $1/N$, assuming that the number of ion channels of each type is $\mathcal{O}(N)$. One can then adapt perturbative methods for solving noise-induced escape problems in jump Markov processes, which involve finding quasi-stationary solutions of the associated master equation using a mixture of Wentzel–Kramers–Brillouin (WKB) methods and matched asymptotics [31]. Here, however, we will develop the WKB method based on a perturbation expansion in a small parameter ϵ, under the assumption that the transition rates of the opening and closing of the ion channels are $\mathcal{O}(1/\epsilon)$ whereas all other characteristic times in the system are $\mathcal{O}(1)$ (on an appropriately chosen time-scale). Such an approach has recently been applied to a variety of stochastic hybrid systems, including spontaneous AP generation in conductance-based neurons [28], gene networks [32] and bistable neural networks [33]. In all of these examples, the calculation of the quasi-stationary solution is considerably more involved than standard jump Markov processes, see also [34, 35]. It should also be noted that a separation of time-scales was previously used by Chow and White [36] in their study of spontaneous APs in the Hodgkin–Huxley model with stochastic ion channels. However, they combined this with a diffusion approximation of the voltage dynamics based on a system-size expansion in $\epsilon = 1/N$. One limitation of the diffusion approximation is that it can lead to exponentially large errors when solving escape problems. This is a consequence of the fact that the (quasi)-stationary probability density for the membrane voltage v takes the large deviation form $p(v) \sim \mathrm{e}^{-\Psi(v)/\epsilon}$ where $\Psi(v)$ is the so-called quasi-potential. The quasi-potential obtained using a diffusion approximation differs from that obtained using the more accurate WKB methods adopted in the current paper, resulting in exponentially large errors when dealing with rare events such as escape from a metastable resting state.

The model of dendritic NMDA spikes has another level of complexity compared to previous models, namely, the maximal conductance of the NMDARs is an exponentially decaying function of time due to the slow unbinding of glutamate, and this plays a crucial role in the termination of spikes. We show how the perturbation analysis of stochastic hybrid systems can be extended to the time-dependent case using a separation of time-scales. We assume that the initial maximum conductance of the NMDARs is sufficiently large so that the membrane is in a bistable regime. For fixed maximum conductance, we first calculate the mean time to escape from the resting state to the depolarized state or vice versa, see figure 2. We then show how to modify the calculation in the presence of a slow exponential decay in the maximum-conductance (due to the slow unbinding of glutamate from NMDARs). Once in the depolarized state, the dendritic spike will terminate in the absence of noise when the membrane loses bistability via a saddle-node bifurcation. We show that in the presence of noise, termination of the dendritic spike can occur before the saddle-node bifurcation, and we calculate the mean time of termination. We also demonstrate that our analytical results agree very well with Monte Carlo simulations of the full model.

The structure of the paper is as follows. We construct our stochastic model of dendritic NMDA spikes in section 2 and show how to recover a deterministic conductance-based model in the limit $\epsilon \to 0$. We then formulate the first passage time (FPT) problem for initiation and termination of spikes in section 3, under the simplifying assumption that the maximal NMDAR conductance is fixed. We then describe the general mathematical framework for calculating the MFPT based on the construction of a quasi-stationary density using WKB methods (section 4) and matched asymptotics (section 5). Note that our analysis is an extension of the theory developed in [28], since we need to take into account two different types of ion channel. Finally, in section 6 we use our analytical expression for the MFPT to determine the mean time for termination of an NMDA spike in the presence of a slowly decaying maximal

NMDAR conductance. We proceed using a stochastic phase-plane analysis based on the study of excitable systems. We also compare the analytical expression for the mean termination time with Monte-Carlo simulations of the full system.

2. Stochastic model of NMDA and Na^+ channels

Let $v(t)$ denote the voltage of a local patch of dendritic membrane containing a mixture of glutamate-bound NMDAR channels and voltage-gated Na^+ channels. Suppose that v evolves according to a deterministic equation of the form

$$C\frac{dv}{dt} = g_x(t)a_x(v)(V_x - v) + \bar{g}_y a_y(v)(V_y - v) + \bar{g}_L(V_L - v), \tag{2.1}$$

where x, y label NMDA and Na^+ channels, respectively, and C is the membrane capacitance. The third term on the right-hand side is an ohmic leak current with maximal conductance $\bar{g}_L$ and membrane reversal potential V_L. The glutamate-bound NMDA receptors act like sodium channels, both having a non-ohmic voltage-dependent conductance such that

$$a_r(v) = \frac{1}{1 + e^{-\gamma_r(v-\kappa_r)}}, \quad r = x, y. \tag{2.2}$$

Here $a_r(v)$ represents the fraction of open ion channels of type r in the limit of fast channel kinetics, see below. The time-dependent deactivation of the NMDA channels following the binding of glutamate is incorporated by taking the maximal conductance of the NMDA receptors to be a slowly decaying function of time t:

$$g_x(t) = \bar{g}_x e^{-t/\tau}, \tag{2.3}$$

where all NMDA receptors are assumed to be glutamate-bound at $t = 0$, and $\tau \gg \tau_x, \tau_y, \tau_L$ with $\tau_r = C/\bar{g}_r$, $r = x, y, L$. For fixed $g_x(t)$, the right-hand side of (2.1) behaves like one of the I–V curves shown in figure 2. Suppose that the maximal NMDA conductance has a value for which the membrane is in a bistable regime. If the deterministic system is in the resting state, then some depolarizing stimulus is needed to switch it to the active state corresponding to a plateau potential, and a subsequent hyperpolarizing stimulus is needed to return the system to the resting state. In practice, termination will occur when the maximal NMDA conductance has reduced sufficiently so that the membrane is no longer bistable.

In this paper, we are interested in how ion channel fluctuations can spontaneously switch the system between the resting and active states, and how this is affected by a slowly changing maximal NMDA conductance. For simplicity, we will initially develop the stochastic analysis in the case of a fixed maximal NMDAR conductance $\bar{g}_x$, and then show how to extend the analysis to the case of a slowly varying conductance for which $\bar{g}_x \to g_x(t) = \bar{g}_x e^{-t/\tau}$. Suppose that each ion channel of type r, $r = x, y$, can exist in either a closed state (C_r) or an open state (O_r). Transitions between the two states are governed by a continuous-time jump Markov process

$$C_r(\text{closed}) \underset{\beta_r}{\overset{\alpha_r(v)}{\rightleftharpoons}} O_r(\text{open}) \tag{2.4}$$

with voltage–dependent transition rate $\alpha_r(v)$. Note that the two-state model is a simplification of more detailed ion channel models, in which there can exist inactivated states and multiple subunits [37]. For example, the Na^+ channel inactivates as well as activates, and consists of multiple subunits, each of which can be in an open state; the channel only conducts when all subunits are open. In order to develop the basic theory, we focus on the simpler two-state model. However, it should be possible to extend the methods presented in this paper to these more complex models, although we do not expect the basic results of the paper to be altered significantly.

Assume for the moment that v is fixed, let $Z_r(t)$ be a discrete random variable taking values $Z_r \in \{C_r, O_r\}$, and set $P^r_z(t) = \text{Prob}[Z_r(t) = z]$. From conservation of probability,

$$P^r_C(t) + P^r_O(t) = 1.$$

The transition rates then determine the probability of jumping from one state to the other in a small interval Δt such that

$$P^r_C(t + \Delta t) = P^r_C(t) - \alpha_r P^r_C(t)\Delta t + \beta_r P^r_O(t)\Delta t.$$

Writing down a similar equation for the open state, dividing by Δt, and taking the limit $\Delta t \to 0$ leads to the pair of equations

$$\frac{dP^r_C}{dt} = -\alpha_r P^r_C + \beta_r P^r_O \tag{2.5}$$

$$\frac{dP^r_O}{dt} = \alpha_r P^r_C - \beta_r P^r_O. \tag{2.6}$$

Now suppose that there are N identical, independent two-state ion channels of each type. (It is straightforward to generalize to the case where the total number of NMDAR and Na^+ channels differ.) In the limit $N \to \infty$ we can reinterpret P^r_C and P^r_O as the mean fraction of closed and open ion channels within the population, and fluctuations can be neglected. After setting $P^r_O = s_r$ and $P^r_C = 1 - s_r$, we obtain the kinetic equation

$$\frac{ds_r}{dt} = \alpha_r(1 - s_r) - \beta_r s_r. \tag{2.7}$$

It turns out the kinetics of glutamate-bound NMDAR channels and Na^+ channels are fast compared to any membrane time constants τ_r. Experimentally, one finds that the time constants for channel kinetics are in the range 100 μs–1 ms (with activation faster than inactivation), whereas membrane time constants are of the order 1–10 ms [38]. This suggests taking $\epsilon \approx 0.1$ (although we will find good agreement between theory and numerics even when ϵ is around one, see section 6). Thus, fixing the time units such that the membrane time constants $\tau_r = \mathcal{O}(1)$, we rescale the transition rates such that

$$\alpha_r, \beta_r \to \alpha_r/\epsilon, \beta_r/\epsilon$$

for $r = x, y$ and some small parameter $\epsilon \ll 1$. (We take the ϵ-scaling of both glutamate-bound NMDAR and Na^+ channels to be the same, which is consistent with physiological findings. It would be interesting mathematically to explore the effects of differences in scaling between the two types of channel, but do not consider this issue further here.) It follows that in the limit $\epsilon \to \infty$, we can make the quasi-steady-state approximation

$$s_r(t) \to a_r(v) \equiv \frac{\alpha_r(v)}{\alpha_r(v) + \beta_r}, \quad r = x, y. \tag{2.8}$$

Comparison with (2.2) implies that

$$\alpha_r(v) = \beta_r \, \mathrm{e}^{\gamma_r(v-\kappa_j)}. \tag{2.9}$$

For $\epsilon > 0$ and a finite number of ion channels, it is necessary to take into account fluctuations in the opening and closing of the ion channels. Suppose that at time t, there are $n_j(t)$ open ion channels of type j with the remaining $N - n_j(t)$ channels closed. Equation (2.1) becomes the piecewise deterministic equation

$$C\frac{\mathrm{d}V}{\mathrm{d}t} = \bar{g}_x \frac{n_x(t)}{N}(V_x - V) + \bar{g}_y \frac{n_y(t)}{N}(V_y - V) + \bar{g}_L(V_L - V), \tag{2.10}$$

which only holds between jumps in the discrete random variables n_x, n_y. The latter are given by the birth–death processes

$$n_r \underset{\omega_+^r(n_r,V)/\epsilon}{\to} n_r + 1, \quad n_r \underset{\omega_-^r(n_r)/\epsilon}{\to} n_r - 1. \tag{2.11}$$

The transition rates are

$$\omega_+^r(n_r, V) = \alpha_r(V)(N - n_r), \quad \omega_-^r(n_r) = \beta_r n_r, \tag{2.12}$$

after rescaling α_j, β_j by a factor $1/\epsilon$. The associated probability density

$$p(v, n_x, n_y, t)\,\mathrm{d}v = \mathbb{P}[v \leqslant V(t) \leqslant v + dv,$$
$$n_x(t) = n_x, n_y(t) = n_y],$$

given an initial condition $V(0) = v_0, n_r(0) = \bar{n}_r$, satisfies the differential Chapman–Kolmogorov (CK) equation (for fixed maximal NMDAR conductance)

$$\frac{\partial p}{\partial t} = -\frac{\partial}{\partial v}[I(v, n_x, n_y)p(v, n_x, n_y, t)] + \frac{1}{\epsilon}\mathbb{L}p(v, n_x, n_y, t), \tag{2.13}$$

where $\mathbb{L} = \mathbb{L}_x + \mathbb{L}_y$,

$$\mathbb{L}_r = (\mathbb{E}_r^+ - 1)\omega_-^r(n_r) + (\mathbb{E}_r^- - 1)\omega_+^r(n_r, V), \tag{2.14}$$

and the $\mathbb{E}_r^\pm$ are ladder operators defined according to $\mathbb{E}_r^\pm F(n_r) = F(n_r \pm 1)$. The drift term takes the form

$$I(v, n_x, n_y) = \frac{n_x}{N} f_x(v) + \frac{n_y}{N} f_y(v) - g(v), \tag{2.15}$$

with $f_x(v) = \bar{g}_x[V_x - v]/C$, $f_y(v) = \bar{g}_y[V_y - v]/C$, $g(v) = -\bar{g}_L[V_L - V]/C$. (In the case of a slowly decaying maximal NMDAR conductance, $\bar{g}_x \to g_x(t)$.)

It is convenient to rewrite equation (2.13) in the form

$$\frac{\partial p}{\partial t} = -\frac{\partial}{\partial v}[I(v, \mathbf{n})p(v, \mathbf{n}, t)] + \frac{1}{\epsilon}\sum_{\mathbf{m}} A(\mathbf{n}, \mathbf{m}; v)p(v, \mathbf{m}), \tag{2.16}$$

where $\mathbf{n} = (n_x, n_y)$ and the matrix A has the non-zero entries

$$A(n_x, n_y, n_x - 1, n_y; v) = \omega_+^x(n_x - 1, v),$$
$$A(n_x, n_y, n_x, n_y - 1; v) = \omega_+^y(n_y - 1, v),$$
$$A(n_x, n_y, n_x + 1, n_y; v) = \omega_-^x(n_x + 1),$$
$$A(n_x, n_y, n_x, n_y + 1; v) = \omega_-^y(n_y + 1),$$
$$A(n_x, n_y, n_x, n_y; v) = -[\omega_-^x(n_x) + \omega_-^y(n_y) + \omega_+^x(n_x, v) + \omega_+^y(n_y, v)].$$

Note that $\sum_{\mathbf{m}} \equiv \sum_{m_x=0}^N \sum_{m_y=0}^N$. For fixed v, A is equivalent to a transition matrix. That is, A is irreducible and has a simple zero eigenvalue with left eigenvector $\mathbf{1}$ and right eigenvector ρ. That is,

$$\sum_{\mathbf{n}} A(\mathbf{n}, \mathbf{m}; v) = 0, \quad \sum_{\mathbf{m}} A(\mathbf{n}, \mathbf{m}; v)\rho(v, \mathbf{m}) = 0. \tag{2.17}$$

The Perron–Frobenius theorem then ensures that all other eigenvalues of $\mathbf{A}(v)$ are negative definite. It follows that, for fixed v, the continuous-time Markov process,

$$\frac{\mathrm{d}p(v, \mathbf{n}, t)}{\mathrm{d}t} = \frac{1}{\epsilon}\sum_{\mathbf{m}} A(\mathbf{n}, \mathbf{m}; v)p(v, \mathbf{m}, t),$$

has a globally attracting steady-state $\rho(v, \mathbf{n})$ with $p(v, \mathbf{n}, t) \to \rho(v, \mathbf{n})$ as $t \to \infty$. The steady-state density ρ can be calculated explicitly using generating functions:

$$\rho(v, n_x, n_y) = \prod_{r=x,y} \frac{N!}{(N - n_r)!n_r!} a_r(v)^{n_r} b_r(v)^{N-n_r} \tag{2.18}$$

with

$$a_r(v) = \frac{\alpha_r(v)}{\alpha_r(v) + \beta_r}, \quad b_r(v) = \frac{\beta_r}{\alpha_r(v) + \beta_r}. \tag{2.19}$$

Using regular perturbation theory, it can be shown that in the limit $\epsilon \to 0$, the probability density $p(v, \mathbf{n}, t) \to C(v, t)\rho(v, \mathbf{n})$ where

$$\rho(v, \mathbf{n})\frac{\partial C}{\partial t} = -\frac{\partial}{\partial v}[\rho(v, \mathbf{n})I(v, \mathbf{n})C(v, t)], \tag{2.20}$$

Summing both sides with respect to n_x and n_y yields the Liouville equation

$$\frac{\partial C}{\partial t} = -\frac{\partial}{\partial v}[F(v)C(v, t)], \tag{2.21}$$

where

$$F(v) = \sum_{\mathbf{n}} \rho(v, \mathbf{n})I(v, \mathbf{n}) = \frac{\bar{n}_x}{N} f_x(v) + \frac{\bar{n}_y}{N} f_y(v) - g(v), \tag{2.22}$$

and $\bar{n}_r$ is the mean number of open channels,

$$\bar{n}_r = \sum_{n_x=1}^N \sum_{n_y=1}^N n_r \rho(v, n_x, n_y) = N a_r(v). \tag{2.23}$$

It follows that in the limit $\epsilon \to 0$ we recover the deterministic voltage equation (see (2.1))

$$\frac{\mathrm{d}v}{\mathrm{d}t} = F(v) = a_x(v)f_x(v) + a_y(v)f_y(v) - g(v) \equiv -\frac{\mathrm{d}\Psi}{\mathrm{d}v}. \tag{2.24}$$

Here $\Psi(v)$ is an effective potential whose minima and maxima correspond to the stable and unstable fixed points of the I–V curves shown schematically in figure 2. Note that the convergence of a stochastic hybrid system to a deterministic system in the $\epsilon \to 0$ limit has been analyzed from a mathematical viewpoint by a number of authors [26, 27, 29, 30, 39].

3. First passage time (FPT) problem and the quasi-stationary approximation

In this section we will assume that the mean-field equation operates in a bistable regime for the given value of $\bar{g}_x$, with a pair of stable fixed points $v_\pm$ and an unstable fixed point v_0, $v_- < v_0 < v_+$. In order to estimate the exponentially

small transition rate from the left to right well (for small ϵ), we place an absorbing boundary at the unstable fixed point v_0 and assume that the system starts in the resting state v_-. (The subsequent time to travel from v_0 to the depolarized state v_+ is insignificant, and can be neglected.) The resulting FPT problem determines the mean time for initiation of a spike (in the absence of an external stimulus). The same analysis can be used to calculate the mean time for termination of a spike (in the absence of glutamate unbinding) by taking the system to start in the right-hand well at v_+. Once we have solved the given FPT problem, we will use stochastic phase-plane analysis in order to determine how a time-dependent NMDAR conductance $g_x(t)$ due to glutamate unbinding combined with noise generates more realistic termination times (see section 6).

In light of the above, the CK equation (2.16) is supplemented by the absorbing boundary conditions

$$p(v_0, \mathbf{n}, t) = 0, \quad \mathbf{n} \in \mathcal{M}, \tag{3.1}$$

where $\mathcal{M}$ is the set of integers (n_x, n_y) for which $I(v_0, \mathbf{n}) < 0$. Let the total number of such elements be $k = |\mathcal{M}|$. The initial condition is taken to be

$$p(v, \mathbf{n}, 0) = \delta(v - v_-)\delta_{\mathbf{n},\mathbf{n}_0}. \tag{3.2}$$

Note that typical values for the reversal potentials are $V_L = -60$ mV, $V_{\rm Na} = 60$ mV and $V_{\rm NMDA} = 0$ mV. Thus, $V_L < V_x < V_y$. From the form of the CK equation (2.16), it follows that if $v_a < V(0) < v_b$ with $v_a = V_L$ and $v_b = V_y$, then $v_a < V(t) < v_b$ for all $t \geqslant 0$. In the absence of a leak current ($\bar{g}_L = 0$), this result holds for $v_a = V_y$ and $v_b = V_x$. In the following we assume that $p(v, n_x, n_y, t) = 0$ for all $v \notin (v_a, v_b)$. Let T denote the (stochastic) FPT for which the system first reaches v_0, given that it started at v_-. The distribution of FPTs is related to the survival probability that the system hasn't yet reached v_0:

$$S(t) \equiv \sum_{\mathbf{n}} \int_{v_a}^{v_0} p(v, \mathbf{n}, t)\, \mathrm{d}v. \tag{3.3}$$

That is, Prob$\{t > T\} = S(t)$ and the FPT density is

$$f(t) = -\frac{\mathrm{d}S}{\mathrm{d}t} = -\sum_{\mathbf{n}} \int_{v_a}^{v_0} \frac{\partial p}{\partial t}(v, \mathbf{n}, t)\, \mathrm{d}v. \tag{3.4}$$

Substituting for $\partial p/\partial t$ using the CK equation (2.16) shows that

$$\begin{aligned} f(t) &= \sum_{\mathbf{n}} \int_{v_a}^{v_0} \frac{\partial [I(v, \mathbf{n})p(v, \mathbf{n}, t)]}{\partial v}\, \mathrm{d}v \\ &= \sum_{\mathbf{n}} I(v_0, \mathbf{n})p(v_0, \mathbf{n}, t). \end{aligned} \tag{3.5}$$

We have used the fact that $\sum_{\mathbf{n}} A(\mathbf{n}, \mathbf{m}; v) = 0$ and $p(v_a, \mathbf{n}, t) = 0$. The FPT density can thus be interpreted as the probability flux $J(v_0, t)$ at the absorbing boundary, since we have the conservation law

$$\sum_{\mathbf{n}} \frac{\partial p(v, \mathbf{n}, t)}{\partial t} = -\frac{\partial J}{\partial v}, \quad J(v, t) = \sum_{\mathbf{n}} I(v, \mathbf{n})p(v, \mathbf{n}, t). \tag{3.6}$$

The FPT problem in the weak noise limit ($\epsilon \ll 1$) has been well studied in the case of Fokker–Planck (FP) equations and master equations, see for example [31, 40–45]. (Typically, ϵ would represent the noise amplitude in the case of a FP equation, whereas $\epsilon = 1/N$ in the case of a master equation with N the number of discrete states.) One of the characteristic features of the weak noise limit is that the flux through the absorbing boundary and the inverse of the mean first passage time (MFPT) $\langle T \rangle$ are exponentially small, that is, $\langle T \rangle \sim \mathrm{e}^{-C/\epsilon}$ for some constant C. This means that standard singular perturbation theory cannot be used to solve the resulting boundary value problem, in which one matches inner and outer solutions of a boundary layer around the point $v = v_0$. Instead, one proceeds by finding a quasi-stationary solution using a WKB approximation. Recently, the WKB method has been extended to a variety of stochastic hybrid systems [28, 32, 33, 46] using a so-called projection method [47]. Here we will use this method to analyze the FPT problem for dendritic spikes.

In order to apply the projection method, it is necessary to assume certain properties of the non self-adjoint linear operator $-\widehat{L}$ on the right-hand side of (2.16) with respect to the Hilbert space of functions $h(v, \mathbf{n})$ with $v \in [v_a, v_0]$ and inner product defined according to

$$\langle h, g \rangle = \sum_{\mathbf{n}} \int_{v_a}^{v_0} h(v, \mathbf{n})g(v, \mathbf{n})\, \mathrm{d}v. \tag{3.7}$$

(i) $\widehat{L}$ has a complete set of eigenfunctions $\phi_r, r = 0, 1, \ldots \hat{N}-1$ with $\hat{N} = (N+1)^2$, and

$$\begin{aligned} \widehat{L}\phi_r(v, \mathbf{n}) &\equiv \frac{\mathrm{d}}{\mathrm{d}v}(I(v, \mathbf{n})\phi_r(v, \mathbf{n})) \\ &\quad - \frac{1}{\epsilon}\sum_{\mathbf{m}} A(\mathbf{n}, \mathbf{m}; v)\phi_r(v, \mathbf{m}) \\ &= \lambda_r \phi_r(v, \mathbf{n}), \end{aligned} \tag{3.8}$$

together with the boundary conditions

$$\phi_r(v_0, \mathbf{n}) = 0, \text{ for } \mathbf{n} \in \mathcal{M}. \tag{3.9}$$

(ii) The real part of the eigenvalues λ_r is positive definite and the smallest eigenvalue λ_0 is real and simple. Thus we can introduce the ordering $0 < \lambda_0 < \mathrm{Re}[\lambda_1] \leqslant \mathrm{Re}[\lambda_2] \leqslant \ldots$.

(iii) λ_0 is exponentially small, $\lambda_0 \sim \mathrm{e}^{-C/\epsilon}$, whereas $\mathrm{Re}[\lambda_r] = \mathcal{O}(1)$ for $r \geqslant 1$. In particular, $\lim_{\epsilon\to 0} \lambda_0 = 0$ and $\lim_{\epsilon\to 0} \phi_0(v, \mathbf{n}) = \rho(v, \mathbf{n})$.

Under the above assumptions, we can introduce the eigenfunction expansion

$$p(v, \mathbf{n}, t) = \sum_{r=0}^{\hat{N}-1} C_r\, \mathrm{e}^{-\lambda_r t}\phi_r(v, \mathbf{n}), \tag{3.10}$$

with $\lambda_0 \ll \mathrm{Re}[\lambda_r]$ for all $r \geqslant 1$. Thus, at large times we have the quasi-stationary approximation

$$p(v, \mathbf{n}, t) \sim C_0\, \mathrm{e}^{-\lambda_0 t}\phi_0(v, \mathbf{n}). \tag{3.11}$$

Substituting such an approximation into equation (3.5) gives

$$f(t) \sim C_0\, \mathrm{e}^{-\lambda_0 t} \sum_{\mathbf{n}} I(v_0, \mathbf{n})\phi_0(v_0, \mathbf{n}), \quad \mathrm{Re}[\lambda_1]t \gg 1, \tag{3.12}$$

Equation (3.8) implies that

$$\sum_{\mathbf{n}}\int_{v_a}^{v_0}\widehat{L}\phi_0(v,\mathbf{n})\,\mathrm{d}v \equiv \sum_{\mathbf{n}} I(v_0,\mathbf{n})\phi_0(v_0,\mathbf{n},t) = \lambda_0\sum_{\mathbf{n}}^{\infty}\phi_0(v,\mathbf{n})\,\mathrm{d}v.$$

In other words,

$$\lambda_0 = \frac{\sum_{\mathbf{n}} I(v_0,\mathbf{n})\phi_0(v_0,\mathbf{n})}{\langle 1,\phi_0\rangle}. \tag{3.13}$$

Combining equations (3.13) and the quasi-stationary approximation (3.12) shows that the (normalized) FPT density reduces to

$$f(t) \sim \lambda_0\,\mathrm{e}^{-\lambda_0 t} \tag{3.14}$$

and, hence, $\langle T\rangle = \int_0^\infty t f(t)\,\mathrm{d}t \sim 1/\lambda_0$.

It remains to obtain an approximation ϕ_ϵ of the principal eigenfunction ϕ_0, which can be achieved using the WKB method as described in section 3.2. This yields a quasi-stationary density that approximates ϕ_0 up to exponentially small terms at the boundary, that is,

$$\widehat{L}\phi_\epsilon = 0, \quad \phi_\epsilon(v_0,\mathbf{n}) = \mathcal{O}(\mathrm{e}^{-C/\epsilon}). \tag{3.15}$$

In order to express λ_0 in terms of the quasi-stationary density ϕ_ϵ, we consider the eigenfunctions of the adjoint operator, which satisfy the equation

$$\widehat{L}^*\xi_s(v,\mathbf{n}) \equiv I(v,\mathbf{n})\frac{\mathrm{d}\xi_s(v,\mathbf{n})}{\mathrm{d}v} - \frac{1}{\epsilon}\sum_{\mathbf{m}} A(\mathbf{m},\mathbf{n};v)\xi_s(v,\mathbf{m}) = \lambda_s\xi_s(v,\mathbf{n}) \tag{3.16}$$

and the boundary conditions

$$\xi_s(v_0,\mathbf{n}) = 0, \quad \mathbf{n}\neq\mathcal{M}. \tag{3.17}$$

Given our assumptions regarding the spectral properties of $\widehat{L}$, the two sets of eigenfunctions form a biorthonormal set with

$$\langle\phi_r,\xi_s\rangle = \delta_{r,s}. \tag{3.18}$$

Now consider the identity

$$\langle\phi_\epsilon,\widehat{L}^*\xi_0\rangle = \lambda_0\langle\phi_\epsilon,\xi_0\rangle. \tag{3.19}$$

Integrating by parts the left-hand side of equation (3.19) picks up a boundary term so that

$$\lambda_0 = -\frac{\sum_{\mathbf{n}}\phi_\epsilon(v_0,\mathbf{n})I(v_0,\mathbf{n})\xi_0(v_0,\mathbf{n})}{\langle\phi_\epsilon,\xi_0\rangle}. \tag{3.20}$$

The calculation of the principal eigenvalue λ_0 thus reduces to the problem of determining the quasi-stationary density ϕ_ϵ and the adjoint eigenfunction ξ_0 using perturbation methods (see below). Once λ_0 has been evaluated, we can then identify the MFPT $\langle T\rangle$ with λ_0^{-1}.

4. WKB method and the quasi-stationary density

We now use the WKB method [31, 42–45] to compute the quasi-stationary density $\boldsymbol{\phi}_\epsilon$. We thus seek a solution of the form

$$\boldsymbol{\phi}_\epsilon(v,\mathbf{n}) = R(v,\mathbf{n})\exp\left(-\frac{\Phi(v)}{\epsilon}\right), \tag{4.1}$$

where $\Phi(v)$ is the quasi-potential. Substituting into the equation $\widehat{L}\phi_\epsilon = 0$, we have

$$\sum_{\mathbf{m}}\left(A(\mathbf{n}\,m;v) + \Phi'(v)\delta_{\mathbf{n},\mathbf{m}}I(v,\mathbf{m})\right)R(v,\mathbf{m}) = \epsilon\frac{\mathrm{d}I(v,\mathbf{n})R(v,\mathbf{n})}{\mathrm{d}v}, \tag{4.2}$$

where $\Phi' = \mathrm{d}\Phi/\mathrm{d}v$. Introducing the asymptotic expansions $R\sim R^{(0)}+\epsilon R^{(1)}$ and $\Phi\sim\Phi_0+\epsilon\Phi_1$, the leading order equation is

$$\sum_{\mathbf{m}} A(\mathbf{n},\mathbf{m};v)R^{(0)}(v,\mathbf{m}) = -\Phi_0'(v)I(v,\mathbf{n})R^{(0)}(v,\mathbf{n}). \tag{4.3}$$

(Note that since $I(v,\mathbf{n})$ is non-zero almost everywhere for $v\in[v_a,v_0]$, we can identify $-\Phi_0'$ and $R^{(0)}$ as an eigenpair of the matrix operator $\widehat{A}(\mathbf{n},\mathbf{m};v) = A(\mathbf{n},\mathbf{m};v)/I(v,\mathbf{n})$ for fixed v.) Positivity of the probability density ϕ_ϵ requires positivity of the corresponding solution $R^{(0)}$. One positive solution is $R^{(0)}=\rho$, for which $\Phi_0'=0$. However, such a solution is not admissible since $\Phi_0=$ constant. It can be proven using linear algebra (see theorem 3.1 of [34]), that since $I(v,\mathbf{n})$ for fixed $v\in[v_a,v_0]$ changes sign as n_x, n_y increase from zero, there exists one other positive solution, such that $\Phi_0'(v)$ has the correct sign and vanishes at the fixed points. Hence, it can be identified as the appropriate WKB solution.

Proceeding to the next order in the asymptotic expansion of equation (4.2),

$$\sum_{\mathbf{m}}\left(A(\mathbf{n},\mathbf{m};v)+\Phi_0'(v)\delta_{\mathbf{n},\mathbf{m}}I(v,\mathbf{m})\right)R^{(1)}(v,\mathbf{m}) = \frac{\mathrm{d}[I(v,\mathbf{n})R^{(0)}(v,\mathbf{n})]}{\mathrm{d}v} - \Phi_1'(v)I(v,\mathbf{n})R^{(0)}(v,\mathbf{n}). \tag{4.4}$$

For fixed v, the matrix operator

$$\bar{A}(\mathbf{n},\mathbf{m};v) = A(\mathbf{n},\mathbf{m};v) + \Phi_0'(v)\delta_{\mathbf{n},\mathbf{m}}I(v,\mathbf{m}) \tag{4.5}$$

on the left-hand side of this equation has a one-dimensional null space spanned by the positive WKB solution $R^{(0)}$. The Fredholm alternative theorem then implies that the right-hand side of (4.4) is orthogonal to the left null vector S of $\bar{A}$. That is, we have the solvability condition

$$\sum_{\mathbf{n}} S(v,\mathbf{n})\left[\frac{\mathrm{d}I(v,\mathbf{n})R^{(0)}(v,\mathbf{n})}{\mathrm{d}v} - \Phi_1'(v)I(v,\mathbf{n})R^{(0)}(v,\mathbf{n})\right] = 0, \tag{4.6}$$

with S satisfying

$$\sum_{\mathbf{n}} S(v,\mathbf{n})\left(A(\mathbf{n},\mathbf{m};v)+\Phi_0'(v)\delta_{\mathbf{n},\mathbf{m}}I(v,\mathbf{m})\right) = 0. \tag{4.7}$$

Given $R^{(0)}$, S and Φ_0, the solvability condition yields the following equation for Φ_1:

$$\Phi_1'(v) = \frac{\sum_{\mathbf{n}} S(v,\mathbf{n})[I(v,\mathbf{n})R^{(0)}(v,\mathbf{n})]'}{\sum_{\mathbf{n}}^{\infty} S(v,\mathbf{n})I(v,\mathbf{n})R^{(0)}(v,\mathbf{n})}. \tag{4.8}$$

Combining the various results, and defining

$$k(v) = \exp\left(-\int_{v_-}^{v}\Phi_1'(y)\,\mathrm{d}y\right), \tag{4.9}$$

gives to leading order in ϵ,

$$\phi_\epsilon(v,\mathbf{n}) \sim \mathcal{A}k(v)\exp\left(-\frac{\Phi_0(v)}{\epsilon}\right)R^{(0)}(v,\mathbf{n}), \tag{4.10}$$

where we choose $\sum_{\mathbf{n}} R^{(0)}(v,\mathbf{n}) = 1$ for all v and $\mathcal{N}$ is the normalization factor,

$$\mathcal{A} = \left[\int_{v_a}^{v_0} k(v)\exp\left(-\frac{\Phi_0(v)}{\epsilon}\right)\right]^{-1}. \tag{4.11}$$

The latter can be approximated using Laplace's method to give

$$\mathcal{A} \sim \frac{1}{k(v_-)}\sqrt{\frac{|\Phi_0''(v_-)|}{2\pi\epsilon}}\exp\left(\frac{\Phi_0(v_-)}{\epsilon}\right). \tag{4.12}$$

4.1. Calculation of Φ_0

Setting $R^{(0)}(v,\mathbf{n}) = \psi(v,n_x,n_y)$ and $\mu = -\Phi_0'(v)$, the eigenvalue equation (4.3) can be written as

$$\begin{aligned}&(N-n_x+1)\alpha_x(v)\psi(v,n_x-1,n_y)\\&\quad+(N-n_y+1)\alpha_y(v)\psi(v,n_x,n_y-1)\\&\quad+(n_x+1)\beta_x\psi(v,n_x+1,n_y)\\&\quad+(n_y+1)\beta_y\psi(v,n_x,n_y+1)\\&\quad-[n_x\beta_x+n_y\beta_y+(N-n_x)\alpha_x(v)\\&\quad+(N-n_y)\alpha_y(v)]\psi(v,n_x,n_y)\\&\quad=\mu\left(\frac{n_x}{N}f_x(v)+\frac{n_y}{N}f_y(v)-g(v)\right)\psi(v,n_x,n_y).\end{aligned} \tag{4.13}$$

Try a normalized positive solution of the form

$$\begin{aligned}\psi(v,n_x,n_y) &= \frac{1}{[1+\Lambda_x(v)]^N}\frac{1}{[1+\Lambda_y(v)]^N}\\&\quad\times\frac{N![\Lambda_x(v)]^{n_x}}{(N-n_x)!n_x!}\cdot\frac{N![\Lambda_y(v)]^{n_y}}{(N-n_y)!n_y!},\end{aligned} \tag{4.14}$$

with $\sum_{n_x,n_y}\psi(v,n_x,n_y) = 1$ for all v. This yields the following equation relating Λ_x, Λ_y and μ:

$$\begin{aligned}&\sum_{p=x,y}\left[\frac{n_p\alpha_p}{\Lambda_p}+\Lambda_p\beta_p(N-n_p)-n_p\beta_p-(N-n_p)\alpha_p\right]\\&\quad=\mu\left(\frac{n_x}{N}f_x+\frac{n_y}{N}f_y-g\right).\end{aligned}$$

Requiring that terms linear in n_x, n_y vanish yields the pair of equations

$$\begin{aligned}\alpha_x\left[\frac{1}{\Lambda_x}+1\right]-\beta_x(\Lambda_x+1) &= \frac{\mu f_x}{N},\\ \alpha_y\left[\frac{1}{\Lambda_y}+1\right]-\beta_y(\Lambda_y+1) &= \frac{\mu f_y}{N},\end{aligned} \tag{4.15}$$

and the remaining terms independent of n_x, n_y give

$$g\mu = N\sum_{p=x,y}[\alpha_p-\beta_p\Lambda_x]. \tag{4.16}$$

Equations (4.15) imply that

$$\frac{f_y}{\Lambda_x}(\alpha_x-\beta_x\Lambda_x)(\Lambda_x+1) = \frac{f_x}{\Lambda_y}(\alpha_y-\beta_y\Lambda_y)(\Lambda_y+1). \tag{4.17}$$

In order to simplify the analysis we set $g = 0$ so that

$$(\alpha_x-\beta_x\Lambda_x) = -(\alpha_y-\beta_y\Lambda_y),$$

that is,

$$\Lambda_y = \frac{\alpha_x+\alpha_y-\beta_x\Lambda_x}{\beta_y}. \tag{4.18}$$

Substituting into (4.17) yields a cubic equation for Λ_x:

$$\begin{aligned}&\left[f_x\beta_y\Lambda_x+(\alpha_x+\alpha_y-\beta_x\Lambda_x)(\Lambda_x(f_x+f_y)+f_y)\right]\\&\quad\times(\alpha_x-\beta_x\Lambda_x)=0.\end{aligned} \tag{4.19}$$

One solution to equations (4.19) and (4.18) is $\Lambda_x = \alpha_x/\beta_x$, $\Lambda_y = \alpha_y/\beta_y$, which reproduces the steady state density $\boldsymbol{\rho}$ corresponding to the zero eigenvalue μ_0. It is also straightforward to check that $\mu = 0$ and $\Lambda_p = \alpha_p/\beta_p$, $p = x, y$ is doubly degenerate at the fixed points $v = v_0, v_-$, for which

$$(\alpha_y(v)+\beta_y)\alpha_x(v)f_x(v)+(\alpha_x(v)+\beta_x(v))\alpha_y(v)f_y(v) = 0. \tag{4.20}$$

In order to determine the positive solution for all v, $v_a < v < v_0$, we rewrite the quadratic part of (4.19) as

$$a\Lambda_x^2+b\Lambda_x+c = 0 \tag{4.21}$$

with

$$\begin{aligned}a &= \beta_x(f_x+f_y)\\ b &= -(\alpha_x+\alpha_y)(f_x+f_y)+\beta_x f_y-f_x\beta_y\\ c &= -(\alpha_x+\alpha_y)f_y.\end{aligned}$$

The roots are $\Lambda_x = \Lambda_x^{\pm}$ with

$$\Lambda_x^{\pm} = -\frac{b}{2a}\pm\frac{\sqrt{b^2-4ac}}{2a}. \tag{4.22}$$

In the given voltage domain, $f_x(v) < 0$, $f_y(v) > 0$ so that the positive root will depend on the sign of $f_x(v)+f_y(v)$. For a given voltage v, there exists a unique positive solution $\boldsymbol{\psi}$ given by (4.14) with $\Lambda_{x,y} = \Lambda_{x,y}^+$ or $\Lambda_{x,y} = \Lambda_{x,y}^-$. Finally, the eigenvalue μ (and hence Φ_0) can be obtained by substituting for Λ_x back into equation (4.15).

4.2. Calculation of Φ_1

Expand out equation (4.7) according to

$$\begin{aligned}&(N-n_x)\alpha_x(v)S(v,n_x+1,n_y)\\&\quad+(N-n_y)\alpha_y(v)S(v,n_x,n_y+1)+n_x\beta_xS(v,n_x-1,n_y)\\&\quad+n_y\beta_yS(v,n_x,n_y-1)-[n_x\beta_x+n_y\beta_y+(N-n_x)\alpha_x(v)\\&\quad+(N-n_y)\alpha_y(v)]S(v,n_x,n_y)\\&=\mu_1(v)\left(\frac{n_x}{N}f_x(v)+\frac{n_y}{N}f_y(v)-g(v)\right)S(v,n_x,n_y).\end{aligned} \tag{4.23}$$

Trying a solution of the form

$$S(v,n_x,n_y) = [\Gamma_x(v)]^{n_x}[\Gamma_y(v)]^{n_y} \tag{4.24}$$

yields

$$\begin{aligned}&(N-n_x)\alpha_x\Gamma_x+(N-n_y)\alpha_y\Gamma_y+n_x\beta_x\Gamma_x^{-1}+n_y\beta_y\Gamma_y^{-1}\\&\quad-\left[(N-n_x)\alpha_x+(N-n_y)\alpha_y+n_x\beta_x+n_y\beta_y\right]\\&\quad=\mu\left(\frac{n_x}{N}f_x+\frac{n_y}{N}f_y-g\right).\end{aligned} \tag{4.25}$$

Γ_x and Γ_y are then determined by canceling terms linear in n_x and n_y, and terms independent of (n_x, n_y). This gives

$$\beta_x\left[\frac{1}{\Gamma_x}-1\right]-\alpha_x(\Gamma_x-1) = \frac{\mu f_x}{N} \tag{4.26}$$

$$\beta_y\left[\frac{1}{\Gamma_y}-1\right]-\alpha_y(\Gamma_y-1)=\frac{\mu f_y}{N} \tag{4.27}$$

$$N\alpha_x(\Gamma_x-1)+N\alpha_y(\Gamma_y-1)=-g\mu. \tag{4.28}$$

Equations (4.26) and (4.27) imply that

$$f_y\left(\beta_x\left[\frac{1}{\Gamma_x}-1\right]-\alpha_x(\Gamma_x-1)\right) = f_x\left(\beta_y\left[\frac{1}{\Gamma_y}-1\right]-\alpha_y(\Gamma_y-1)\right). \tag{4.29}$$

Again let us set $g=0$ so that

$$\Gamma_y=\frac{(\alpha_x+\alpha_y)-\alpha_x\Gamma_x}{\alpha_y}. \tag{4.30}$$

Substituting for Γ_y into (4.29) gives a cubic for Γ_x:

$$[(f_y\beta_x+\Gamma_x\alpha_x(f_x+f_y))(\alpha_x(1-\Gamma_x)+\alpha_y) +f_x\beta_y\alpha_x\Gamma_x)](1-\Gamma_x)=0. \tag{4.31}$$

The root $\Gamma_x=1,\Gamma_y=1$ corresponds to the solution $S(v,\mathbf{n})\equiv\mathbf{1}$ associated with the zero eigenvalue $\mu=0$. We also require that $\mu=0$ and $S=1$ at a fixed point for which (4.20) holds. Imposing the fixed point condition, equation (4.31) reduces to

$$(f_y\beta_x+\Gamma_x\alpha_x(f_x+f_y))\alpha_x(1-\Gamma_x)^2=0, \tag{4.32}$$

which confirms the existence of a double root. For general v, the quadratic factor in equation (4.31) takes the form

$$a\Gamma_x^2+b\Gamma_x+c=0, \tag{4.33}$$

with

$$\begin{aligned}a&=\alpha_x^2(f_x+f_y),\\ b&=f_y\alpha_x\beta_x-f_x\alpha_x\beta_y-\alpha_x(\alpha_x+\alpha_y)(f_x+f_y),\\ c&=-(\alpha_x+\alpha_y)\beta_y f_x.\end{aligned}$$

Again, only one of the two remaining solutions has positive Γ_x, assuming that $f_x<0$, $f_y>0$ and $f_x+f_y>0$.

5. Calculation of principal eigenvalue using matched asymptotics

In order to evaluate the principal eigenvalue using equation (3.20), we need both the quasi-stationary density $\phi_\epsilon(v,\mathbf{n})$ and the adjoint eigenfunction $\xi_0(v,\mathbf{n})$. The latter can be determined using singular perturbation methods[28, 34, 46]. Since λ_0 is exponentially small in ϵ, equation (3.16) yields the leading order equation

$$\epsilon I(v,\mathbf{n})\frac{\mathrm{d}\xi_0(v,\mathbf{n})}{\mathrm{d}v}+\sum_{\mathbf{m}}A(\mathbf{m},\mathbf{n};v)\xi_0(v,\mathbf{m})=0, \tag{5.1}$$

supplemented by the absorbing boundary condition

$$\xi_0(v_0,\mathbf{n})=0,\quad \mathbf{n}\notin\mathcal{M}. \tag{5.2}$$

A first attempt at obtaining an approximate solution that also satisfies the boundary conditions is to construct a boundary layer in a neighborhood of the unstable fixed point v_0 by performing the change of variables $v=v_0-\epsilon z$ and setting $Q(z,\mathbf{n})=\xi_0(v_0-\epsilon z)$. Equation (5.1) then becomes

$$I(v_0,\mathbf{n})\frac{\mathrm{d}Q(z,\mathbf{n})}{\mathrm{d}z}+\sum_{\mathbf{m}}A(\mathbf{m},\mathbf{n};v_0)Q(z,\mathbf{m})=0. \tag{5.3}$$

This inner solution has to be matched with the outer solution $\xi_0(v,\mathbf{n})=1$, which means that

$$\lim_{z\to\infty}Q(z,\mathbf{n})=1 \tag{5.4}$$

for all $\mathbf{n}$. Consider the eigenvalue equation

$$\sum_{\mathbf{n}}\left(A(\mathbf{n},\mathbf{m};v)-\mu_r(v)\delta_{\mathbf{n},\mathbf{m}}I(v,\mathbf{m})\right)S_r(v,\mathbf{n})=0. \tag{5.5}$$

We take $S_0(v,\mathbf{n})=1$ so that $\mu_0=0$ and set $S_1(v,\mathbf{n})=S(v,\mathbf{n})$, $\mu_1(v)=-\Phi_0'(v)$, where S satisfies equation (4.7). We then introduce the eigenfunction expansion

$$Q(z,\mathbf{n})=c_0+\sum_{r=1}^{\hat{N}-1}c_rS_r(v_0,\mathbf{n})\,\mathrm{e}^{-\mu_r(v_0)z}. \tag{5.6}$$

In order that the solution remains bounded as $z\to\infty$ we require that $c_r=0$ if $\mathrm{Re}[\mu_r(v_0)]>0$. The boundary conditions (5.2) generate a system of $\widehat{N}-k$ linear equations for $\widehat{N}$ unknown coefficients c_r. One of the unknowns in determined by matching the outer solution, which suggests that there are $k-1$ eigenvalues with negative real part. The eigenvalues are ordered so that $\mathrm{Re}[\mu_r(v_0)]<0$ for $r=\widehat{N}-k+1,\ldots,\widehat{N}-1$ and $\mathrm{Re}[\mu_r(v_0)]\geqslant 0$ for $r=0,\ldots,\widehat{N}-k$.

There is, however, one problem with the above eigenfunction expansion, namely, that $\mu_1(v_0)=0$ so that the zero eigenvalue is degenerate. (The vanishing of $\mu_1=-\Phi_0'$ at fixed points follows from theorem 3.1 of [34].) Hence, the solution needs to include a secular term involving the generalized eigenvector $\widehat{S}$,

$$\sum_{\mathbf{n}}A(\mathbf{n},\mathbf{m};v_0)\widehat{S}(v_0,\mathbf{n})=-I(v_0,\mathbf{m}). \tag{5.7}$$

The Fredholm alternative theorem ensures that $\widehat{S}$ exists and is unique, since the stationary density $\rho(v_0,\mathbf{m})$ is the right null vector of $A(\mathbf{n},\mathbf{m};v_0)$, and

$$\sum_{\mathbf{n}}\rho(v_0,\mathbf{n})I(v_0,\mathbf{n})\equiv F(v_0)=0.$$

In component form with $(\boldsymbol{\zeta}_0)_j=\zeta(n_x,n_y)$,

$$\begin{aligned}&(N-n_x)\alpha_x(v_0)\zeta(n_x+1,n_y)+n_x\beta_x\zeta(n_x-1,n_y)\\ &\quad+(N-n_y)\alpha_y(v_0)\zeta(n_x,n_y+1)+n_y\beta_y\zeta(n_x,n_y-1)\\ &\quad-((N-n_x)\alpha_x(v_0)+n_x\beta_x+(N-n_y)\alpha_y(v_0)\\ &\quad+n_y\beta_y)\zeta(n_x,n_y)\\ &=g(v_0)-\frac{n_x}{N}f_x(v_0)-\frac{n_y}{N}f_y(v_0).\end{aligned} \tag{5.8}$$

Try a solution of the form

$$\zeta_n=An_x+Bn_y. \tag{5.9}$$

Equating terms linear in n_x, n_y and terms independent of n_x, n_y gives

$$\begin{aligned}A\alpha_x+B\alpha_y&=\frac{g}{N}\\ A(\alpha_x+\beta_x)=\frac{f_x}{N},&\quad B(\alpha_y+\beta_y)=\frac{f_y}{N}.\end{aligned}$$

Using the fixed point equation shows that

$$\zeta(n_x, n_y) = \frac{f_x}{\alpha_x + \beta_x}\frac{n_x}{N} + \frac{f_y}{\alpha_y + \beta_y}\frac{n_y}{N}. \tag{5.10}$$

The solution for $Q(z, \mathbf{n})$ is now

$$Q(z, \mathbf{n}) = c_0 + c_1(\widehat{S}(v_0, \mathbf{n}) - z) + \sum_{r=2}^{\hat{N}-k} c_r S_r(v_0, \mathbf{n})\, \mathrm{e}^{-\mu_r(v_0)z}. \tag{5.11}$$

The presence of the secular term means that the solution is unbounded in the limit $z \to \infty$, which means that the inner solution cannot be matched with the outer solution. One way to remedy this situation is to introduce an alternative scaling in the boundary layer of the form $v = v_0 - \epsilon^{1/2}z$, as detailed in [46]. One can then eliminate the secular term $-c_1 z$ and show that

$$c_1 \sim \sqrt{\frac{2|\Phi_0''(v_0)|}{\pi}} + \mathcal{O}(\epsilon^{1/2}), \qquad c_r = \mathcal{O}(\epsilon^{1/2}) \quad \text{for } r \geqslant 2. \tag{5.12}$$

It turns out that we only require the first coefficient c_1 in order to evaluate the principal eigenvalue λ_0 using equation (3.20). This follows from equations (4.3) and (5.5), and the observation that the left and right eigenvectors of the matrix $\widehat{A}(\mathbf{n}, \mathbf{m}; v) = A(\mathbf{n}, \mathbf{m}; v)/I(v, \mathbf{n})$ are biorthogonal. In particular, since the quasi-stationary approximation ϕ_ϵ is proportional to $R^{(0)}$, see equation (4.10), it follows that ϕ_ϵ is orthogonal to all eigenvectors S_r, $r \neq 1$. Simplifying the denominator of equation (3.20) by using the outer solution $\xi_0 \sim 1$, we obtain

$$\begin{aligned}\lambda_0 &\sim -\frac{\sum_{\mathbf{n}} \xi_0(v_0, \mathbf{n}) I(v_0, \mathbf{n})\phi_\epsilon(v_0, \mathbf{n})}{\langle \phi_\epsilon, 1\rangle} \\ &\sim c_1 \frac{k(v_0)B(v_0)}{k(v_-)}\sqrt{\frac{|\Phi''(v_-)|}{2\pi}} \\ &\quad \times \exp\left(-\frac{\Phi_0(v_0) - \Phi_0(v_-)}{\epsilon}\right),\end{aligned} \tag{5.13}$$

with

$$B(v_0) = -\sum_{\mathbf{n}} \widehat{S}(v_0, \mathbf{n}) v(v_0, \mathbf{n})\rho(v_0, \mathbf{n}). \tag{5.14}$$

Substituting for c_1, we obtain our final result

$$\begin{aligned}\lambda_0 &\sim \frac{1}{\pi}\frac{k(v_0)B(v_0)}{k(v_-)}\sqrt{\Phi_0''(v_-)|\Phi_0''(v_0)|} \\ &\quad \times \exp\left(-\frac{\Phi_0(v_0) - \Phi_0(v_-)}{\epsilon}\right).\end{aligned} \tag{5.15}$$

Repeating the analysis for transition from the depolarized state to the resting state gives

$$\begin{aligned}\lambda_0 &\sim \frac{1}{\pi}\frac{k(v_0)B(v_0)}{k(v_+)}\sqrt{\Phi_0''(v_+)|\Phi_0''(v_0)|} \\ &\quad \times \exp\left(-\frac{\Phi_0(v_0) - \Phi_0(v_+)}{\epsilon}\right).\end{aligned} \tag{5.16}$$

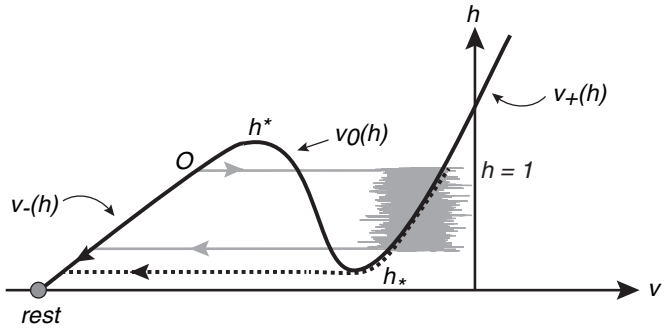

Figure 3. Sketch of nullclines in the deterministic planar dendritic spike model with v denoting membrane potential and h keeping track of the fraction of glutamate-bound NMDARs. The v nullcline is cubic-like with three branches $v_\pm(h)$ and $v_0(h)$. In the given diagram there is a single, stable fixed point on the left-hand branch. In the stochastic version of the model, a dendritic spike is initiated by stimulus-induced jump to the right-hand branch $v_+(h)$. This is followed by a stochastic trajectory in which the slow variable h moves down the nullcline until it undergoes a noise-induced transition back to the left-hand branch $v_-(h)$ before the knee at $h = h_*$. In the deterministic case, the return transition occurs at the knee (dashed curve).

6. Stochastic phase-plane analysis

In the above analysis of dendritic NMDA spikes, the maximal NMDA conductance was held fixed at $\bar{g}_x$. However, following stimulation at time $t = 0$, the maximal conductance slowly decays according to equation (2.3). Thus, the deterministic model becomes the planar dynamical system

$$\begin{aligned}\frac{\mathrm{d}v}{\mathrm{d}t} &= ha_x(v)(V_x - v)/\tau_x + a_y(v)(V_y - v)/\tau_y + (V_L - v)/\tau_L \\ &\equiv J(v, h),\end{aligned} \tag{6.1}$$

$$\frac{\mathrm{d}h}{\mathrm{d}t} = -\frac{h}{\tau}, \quad h(0) = 1. \tag{6.2}$$

We will assume a separation of time-scales for which $\tau_j \ll \tau$, that is, the membrane time constants are smaller than the decay time due to the unbinding of glutamate from NMDARs. If the variation in the maximal NMDAR conductance is included, then the membrane acts like an excitable system rather than a bistable system on long time-scales. For there is now only a single fixed point, which is given by the resting state. Since the resting state is hyperpolarized, we expect most of the NMDAR channels to be blocked by Mg^{2+} even when bound to glutamate. Thus, Na^+ channels play the major role in the initiation of a dendritic spike, so the analysis of previous sections still holds. On the other hand, the decay of h is expected to play an important role in the termination of the spike. Following along analogous lines to the analysis of Ca^{2+} sparks by Hinch [48], we can analyze spike termination by combining the theory of stochastic transitions with the classical phase-plane analysis of slow–fast excitable systems.

In figure 3 we sketch the nullclines of the deterministic system in a parameter regime where there is a single, stable fixed point $(v^*, 0)$. The fast variable v has a cubic-like nullcline (along which $\dot{v} = 0$) and the slow variable h has the axis $h = 0$ as its nullcline (along which $\dot{h} = 0$). We assume that the nullclines have a single intersection point at $(v^*, 0)$. This

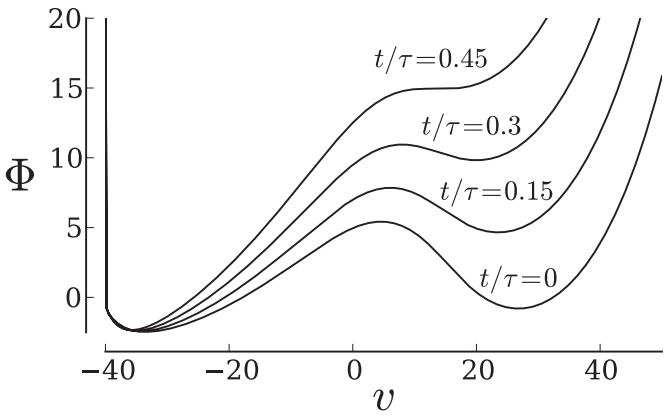

Figure 4. The effective potential $\Phi(v,t)$ plotted as a function of voltage v for different times t, showing the effect of glutamate slowly unbinding from NMDA receptors. At $t/\tau \approx 0.45$, a bifurcation occurs, where the right well vanishes. For $t/\tau > 0.45$ the system is monostable, and as $t \to \infty$ the voltage returns to the resting state. Parameter values are $N = 5$, $\beta_x = \beta_y = 1$ ms^{-1}, $C = 0.8$ mF, $g_x = 0.12$ mΩ^{-1}, $g_y = 0.2$ mΩ^{-1}, $g_L = 0$, $v_x = 80$ mV, $v_y = -40$ mV, $\gamma_x = 0.25$ mV^{-1}, $\kappa_x = 8$ mV, $\gamma_y = 0.03$ mV^{-1}, and $\kappa_y = 30$ mV.

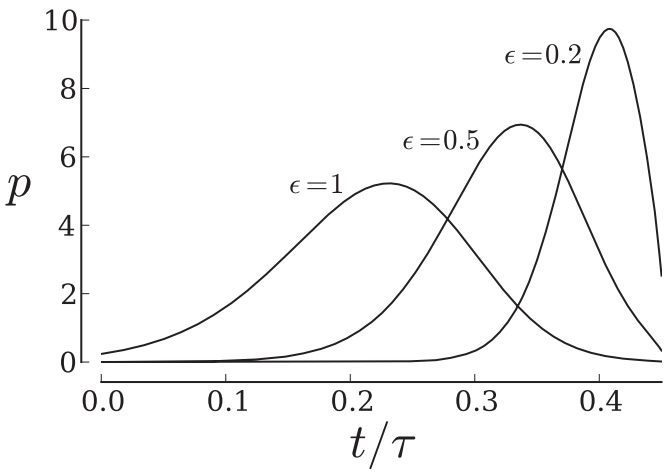

Figure 5. The first passage time density function $p(t)$ for different values of ϵ. Parameter values are the same as figure 4.

corresponds to a fixed point of the system, which we identify with the resting state. For a finite range of values of h, there exist three solutions of the equation $J(v,h) = 0$, which we denote by $v_-(h)$, $v_0(h)$ and $v_+(h)$. Whenever these solutions coexist, we choose the ordering $v_-(h) \leqslant v_0(h) \leqslant v_+(h)$. Let h_* denote the minimal value of h for which $v_+(h)$ exists, and let h^* denote the maximal value of h for which $v_-(h)$ exists. Suppose that at $t = 0$, the NMDARs have their maximal conductance ($h = 1$) and a dendritic spike is initiated by an external stimulus (point O in figure 3). This induces a fast transition from the left-hand to the right-hand v-nullcline according to $v_-(1) \to v_+(1)$. The system then moves down the right-hand nullcline $v_+(h)$ with $h(t) = \mathrm{e}^{-t/\tau}$. In the absence of noise, there is a return transition to the left-hand branch at the knee where $h = h_*$. On the other hand, in the full stochastic model we expect there to be a noise-induced transition back to $v_-(h)$ before reaching the knee. Suppose that at time t the dendritic spike has not yet terminated and set $v_\pm(t) = v_\pm(h(t))$. Using a separation of time-scales, we can estimate the rate of transition $v_+(t) \to v_-(t)$ for fixed t using our solution (5.16):

$$\lambda_0(t) \sim \frac{1}{\pi}\frac{k(v_0(t),t)}{k(v_+(t),t)}B(v_0(t),t)\sqrt{\Phi_0''(v_+(t),t)|\Phi_0(v_0(t),t)|} \times \exp\left(-\frac{[\Phi_0(v_0(t),t)-\Phi_0(v_+(t),t)]}{\epsilon}\right), \tag{6.3}$$

Here the time-dependent functions $\Phi_0(v,t)$, $k(v,t)$ and $B(v,t)$ are obtained by making the replacement $f_x(v) \to f_x(v,t) \equiv \bar{g}_x h(t)[V_x - v]/C$ in the various results derived in sections 4 and 5. In figure 4 we plot the analytically determined potential $\Phi(v,t)$ as a function of voltage v for various times t. It can be seen that for sufficiently small t, Φ is a double-well potential consistent with the initial condition that the system is bistable for fixed $h = 1$. However, as t increases (so h decreases), the potential undergoes a bifurcation to become monostable, reflecting the existence of only a resting state when $h = 0$.

We can now calculate the distribution of dendritic spike durations T. Let $P(s) = \mathbb{P}(T > s)$ and introduce the spike duration probability density

$$p(s) = -\frac{\mathrm{d}P}{\mathrm{d}s}.$$

The probability that a spike terminates in an infinitesimal time interval δs is $\lambda_0(s)\delta s$, so that

$$P(s+\delta s) = P(s)(1-\lambda_0(s)\delta s).$$

Taking the limit $\delta s \to 0$ and integrating gives $P(s) = \exp\left(-\int_0^s \lambda_0(t)\,\mathrm{d}t\right)$, and hence

$$p(s) = \lambda_0(s)\exp\left(-\int_0^s \lambda_0(t)\,\mathrm{d}t\right). \tag{6.4}$$

In figure 5 we plot the FPT density p as a function of time for various ϵ. It can be seen that as ϵ decreases, so that the rate at which the NMDA and Na^+ channels open and close becomes faster, the mean termination time increases. This is consistent with the stochastic phase-plane analysis shown in figure 3 and the observation that we recover the deterministic model in the limit $\epsilon \to 0$. Also note that after time averaging $\lambda_0(t)$, the MFPT is comparable to the decay time τ, indicative of the crucial role of glutamate unbinding in spike termination. In figure 6 we compare our analytical results for the mean termination time T with Monte-Carlo simulations of the full stochastic model. (Details of how we perform the simulations can be found in [28].) It can be seen that there is good agreement between theory and numerics even when the perturbation parameter $\epsilon = 1$. There are two factors contributing to the accuracy of our calculation: the level of noise ϵ and the value of τ. Clearly, our perturbation analysis will break down when ϵ becomes too large. The dependence on τ reflects the fact that the approximation (6.4) in the case of a time-dependent eigenvalue $\lambda_0(t)$ breaks down if the survival probability $P(t)$ remains large at the saddle-node bifurcation point. This can occur for sufficiently small ϵ and τ, as illustrated in figure 7. Finally, note that we choose parameter values such that the time constants τ_x, τ_y are around 1 ms and $\tau = 10^3$ is around 100 ms, which is consistent with physiological measurements [9].

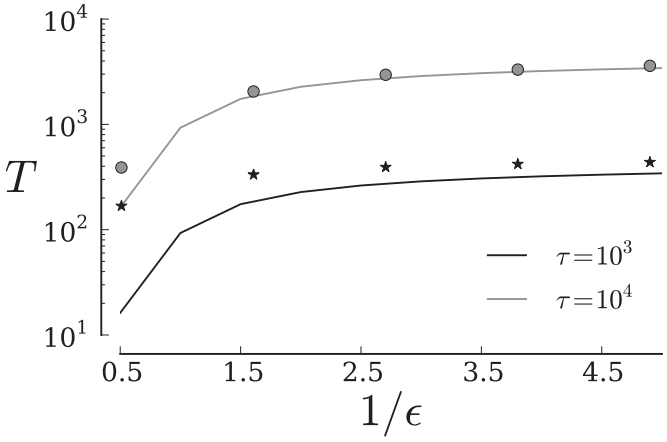

Figure 6. The mean first passage time for the system to leave the active state and return to the resting state plotted as a function of ϵ. Solid curves show the quasi-stationary approximation for $\tau = 10^3$ (black curve) and $\tau = 10^4$ (gray curve). The corresponding results from 20 averaged Monte-Carlo simulations are indicated by $*$ and $\circ$, respectively. Other parameter values are the same as in figure 4.

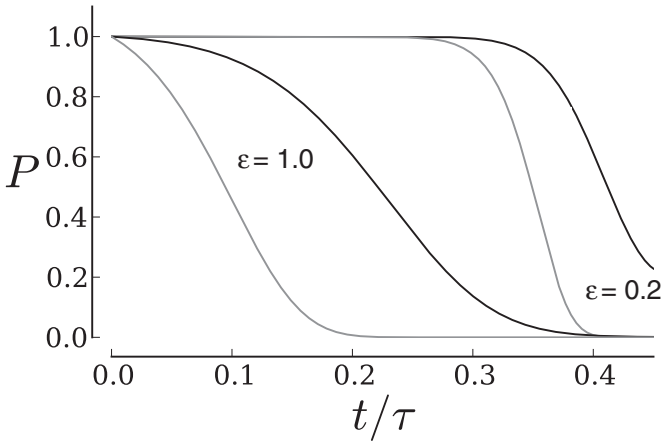

Figure 7. The survival probability $P(t)$ for two different values of ϵ with $\tau = 10^3$ (black curves) and $\tau = 10^4$ (gray curves). Other parameter values are the same as in figure 4. It can be seen that $P(t)$ for fixed t decreases as τ or ϵ decreases.

7. Discussion

In recent years there has been growing interest in understanding how fluctuations in the opening and closing of ion channels affects classical conductance-based models of neural excitability. Almost all of this work has focused on the dynamics of Na^+ and K^+ channels involved in the generation of action potentials. In this paper, we considered another important example of neural excitability, namely, the occurrence of spikes in thin dendrites mediated by Na^+ and glutamatergic NMDA channels. Although the initiation of such a spike has certain similarities with standard APs, the mechanism of termination is very different, involving the slow unbinding of glutamate from NMDA receptors rather than the activation of K^+ channels (and deactivation of Na^+ channels). We extended previous work on the quasi-stationary (multiple time scale) analysis of membrane voltage fluctuations in the presence of channel noise in order to take into account glutamate unbinding. This required an additional separation of time scales and the use of stochastic phase-plane analysis. We calculated the mean termination time of a spike under physiologically reasonable conditions and established that our analysis agrees well with numerical simulations of the full stochastic model.

What are the possible biological implications of our work from the perspective of dendritic spikes? One general result is that it is not necessary for the number of ion channels N to be large in order to analyze the effects of channel noise (using a system-size expansion, say), provided that there is some form of separation of time scales. This could be particularly important in the case of dendritic spikes, since they occur in thin dendrites where the density of ion channels could be quite low. Another aspect of our work is that we identify an explicit mechanism for termination of a dendritic spike based on a combination of slow/fast analysis and channel fluctuations. In addition to addressing the particular biophysical phenomenon of dendritic spikes, our work further demonstrates the applicability of WKB methods and quasi-stationary analysis to stochastic hybrid systems. There is a rapidly expanding list of biological phenomena for which a continuous process couples to a discrete Markov process, including neural excitability (membrane voltage/ion channel gating), calcium sparks (calcium concentration/ion channel gating), gene networks (protein concentration/promoters), and stochastic neural networks (population synaptic currents/spiking activity). All of these systems exhibit bistability and thus require the use of methods similar to those presented here.

We conclude by noting that there is an important connection between WKB methods and large deviation theory [49, 50]. That is, it has been established within the context of chemical master equations and stochastic differential equations that the quasi-potential obtained using the WKB method can be interpreted as an effective action evaluated along a path of maximum likelihood for the underlying stochastic process. This is particularly important when considering escape problems in higher-dimensional systems. A mathematical formulation of large deviation theory has recently been developed for a stochastic hybrid system [39]. It would be interesting in future work to develop the connection with our WKB analysis. One possible approach would be to construct a path-integral representation of solutions to the corresponding Chapman–Kolmogorov equation by analogy with the Doi–Peliti path-integral developed for chemical master equations [51–53].

Acknowledgments

PCB was supported by the National Science Foundation (DMS-1120327) and JMN by the Mathematical Biosciences Institute and the National Science Foundation undergrant DMS 0931642.

References

[1] Stuart G, Spruston N and Hausser M (eds) 2007 *Dendrites* (Oxford: Oxford University Press)
[2] Stuart G J and Sakmann B 1994 *Nature* **367** 69–72
[3] Magee J C and Johnston D 1995 *J. Physiol.* **487** 67–90

[4] Sjostrom P J, Rancz E A, Roth A and Hausser M 2008 *Physiol. Rev.* **88** 769–840
[5] Kim H G and Connors B W 1993 *J. Neurosci.* **13** 5301–11
[6] Schiller J, Schiller Y, Stuart G and Sakmann B 1997 *J. Physiol.* **505** 605–16
[7] Golding N L, Staff N P and Spruston N 2002 *Nature* **418** 326–31
[8] Larkum M E, Zhu J J and Sakmann B 1999 *Nature* **398** 338–41
[9] Schiller J, Major G, Koester H J and Schiller Y 2000 *Nature* **404** 285–9
[10] Rhodes P 2006 *J. Neurosci.* **26** 6704–15
[11] Major G, Polsky A, Denk W, Schiller J and Tank D W 2008 *J. Neurophysiol.* **99** 2584–601
[12] Larkum M E, Nevian T, Sandler M, Polsky A and Schiller J 2009 *Science* **325** 756–60
[13] Antic S D, Zhou W L, Moore A R, Short S M and Ikonomu K D 2010 *J. Neurosci. Res.* **88** 2991–3001
[14] Mayer M L, Westbrook G L and Guthrie P B 1984 *Nature* **309** 261–3
[15] Nowak L, Bregestovski P, Ascher P, Herbet A and Prochiantz A 1984 *Nature* **307** 462–5
[16] Kiehn O and Eken T 1998 *Curr. Opin. Neurobiol.* **8** 746–52
[17] Lisman J E, Fellous J M and Wang X J 1998 *Nature Neurosci.* **1** 273–5
[18] Durstewitz D and Seamans J K 2006 *Neuroscience* **139** 119–33
[19] Seung H S, Lee D D, Reis B Y and Tank D W 2000 *Neuron* **26** 259–71
[20] Milojkovic B A, Radojicic M S, Goldman-Rakic P S and Antic S D 2004 *J. Physiol.* **558** 193–211
[21] Jahr C and Stevens C 1990 *J. Neurosci.* **10** 1830–7
[22] Shoemaker P A 2011 *Neurocomputing* **74** 3058–71
[23] Moradi K, Moradi K, Gamjkhani M, Hajihasani M, Gharibzadeh S and Kaka G 2012 *J. Comput. Neurosci.* **34** 521–31
[24] Sanders H, Berends M, Major G, Goldman M S and Lisman J E 2013 *J. Neurosci.* **33** 424–9
[25] Groff J R, DeRemigio H and Smith G D 2009 Markov chain models of ion channels and calcium release sites *Stochastic Methods in Neuroscience* (Oxford: Oxford University Press) chapter 2 pp 29–64
[26] Pakdaman K, Thieullen M and Wainrib G 2010 *J. Appl. Prob.* **24** 1
[27] Buckwar E and Riedler M G 2011 *J. Math. Biol.* **63** 1051–93
[28] Keener J P and Newby J M 2011 *Phy. Rev.* E **84** 011918
[29] Wainrib G, Thieullen M and Pakdaman K 2012 *J. Comput. Neurosci.* **32** 327–46
[30] Pakdaman K, Thieullen M and Wainrib G 2012 *Stochastic Process. Appl.* **122** 2292–318
[31] Schuss Z 2010 *Theory and Applications of Stochastic Processes: an Analytical Approach (Applied Mathematical Sciences* vol 170*)* (New York: Springer)
[32] Newby J M 2012 *Phys. Biol.* **9** 026002
[33] Bressloff P C and Newby J M 2013 *SIAM J. Appl. Dyn. Sys.* **12** 1394–435
[34] Newby J M and Keener J P 2011 *Multiscale Model. Simul.* **9** 735–65
[35] Newby J and Chapman J 2012 *J. Math. Biol.* In press
[36] Chow C C and White J A 1996 *Biophys. J.* **71** 3013–21
[37] Goldwyn Joshua H and Shea-Brown E 2011 *PLoS Comput. Biol.* **7** e1002247
[38] Byrne J H and Roberts J L 2004 *From Molecules to Networks: An Introduction to Cellular and Molecular Neuroscience* (Amsterdam: Elsevier)
[39] Faggionato A, Gabrielli D and Crivellari M 2010 *Markov Process. Relat. Fields* **16** 497–548
[40] Ludwig D 1975 *SIAM Rev.* **17** pp 605–40
[41] Matkowsky B J and Schuss Z 1977 *SIAM J. Appl. Math.* **33** 365–82
[42] Hanggi P, Grabert H, Talkner P and Thomas H 1984 *Z. Phys.* B **28** 135
[43] Naeh T, Klosek M M, Matkowsky B J and Schuss Z 1990 *SIAM J. Appl. Math.* **50** 595–627
[44] Dykman M I, Mori E, Ross J and Hunt P M 1994 *J. Chem. Phys.* A **100** 5735–50
[45] Maier R S and Stein D L 1997 *SIAM J. Appl. Math.* **57** 752–90
[46] Newby J M, Bressloff P C and Keener J P 2013 *Phys. Rev. Lett.* **111** 128101
[47] Ward M J and Lee J 1995 *Stud. Appl. Math.* **94** 271–326
[48] Hinch R 2004 *Biophys. J.* **86** 1293–307
[49] Freidlin M I and Wentzell A D 1998 *Random Perturbations of Dynamical Systems* 2nd ed (New York: Springer)
[50] Touchette H 2009 *Phys. Rep.* **478** 1–69
[51] Doi M 1976 *J. Phys. A: Math. Gen.* **9** 1465–77
[52] Doi M 1976 *J. Phys. A: Math. Gen.* **9** 1479–95
[53] Peliti L 1985 *J. Physique* **46** 1469–83